

Insulin-like Growth Factor Binding Protein6 Associated with Neuronal Apoptosis Following Intracerebral Hemorrhage in Rats

Qijun Dai¹ · Peipei Jiang¹ · Yang Gu¹ · Lin Zhu¹ · Haifeng Dai¹ · Zhigang Yao¹ · Hua Liu¹ · Xiaoping Ma¹ · Chengwei Duan² · Lianxia Qu¹

Received: 4 August 2016 / Accepted: 1 December 2016 / Published online: 2 January 2017
© Springer Science+Business Media New York 2016

Abstract The insulin-like growth factor (IGF) system is linked to CNS pathological states. The functions of IGFs are modulated by a family of binding proteins termed insulin-like growth factor binding proteins (IGFBPs). Here, we demonstrate that IGFBP-6 may be associated with neuronal apoptosis in the processes of intracerebral hemorrhage (ICH). We obtained a significant upregulation of IGFBP-6 in neurons adjacent to the hematoma following ICH with the results of Western blot, immunohistochemistry, and immunofluorescence. Increasing IGFBP-6 level was found to be accompanied by the upregulation of Bax, Bcl-2, and active caspase-3. Besides, IGFBP-6 co-localized well with active caspase-3 in neurons, indicating its potential role in neuronal apoptosis. Knocking down IGFBP-6 by RNA-interference in PC12 cells reduced active caspase-3 expression. Thus, IGFBP-6 may play a role in promoting the brain secondary damage following ICH.

Keywords Intracerebral hemorrhage · IGF · IGFBP-6 · Neuronal apoptosis · Rat

Introduction

Intracerebral hemorrhage (ICH) is a detrimental type of stroke with no specific treatments. ICH is characterized by bleeding when a blood vessel ruptures, subsequently causing neuroinflammatory responses to blood components (Hammond et al. 2014). Multiple resources have illustrated the significant progress in understanding the pathophysiology of ICH, but the current interventions have failed to improve outcomes (Ke et al. 2015; Leclerc et al. 2015). Pathologic changes of ICH include primary and secondary damage. The primary damage is usually caused by mechanical damage; the secondary damage contains lots of parallel pathways, causing the disability or even the death ultimately (Aronowski and Zhao 2011; Liu et al. 2016; Xi et al. 2006). Among the process of the pathologic changes, neuronal apoptosis is a crucial event including pro-apoptotic activation and anti-apoptotic modulation (Chen et al. 2015). Here, we try to explore the mechanisms underlying ICH to improve the outcomes of treatments toward neurological diseases.

The insulin-like growth factor (IGF) system is polypeptides, comprising a family of the ligands IGF-1 and IGF-2 (Haramoto et al. 2014). IGF-1 and IGF-2 play essential role in the regulation of cell growth, differentiation, proliferation, morphogenesis, growth, and apoptosis (Annunziata et al. 2011; Chao and D'Amore 2008; Konermann et al. 2013). IGF-1 plays an important role in protection from apoptosis and regulation of development and growth (Malandrakis et al. 2016). IGF-2 has been showed to have prognostic relevance in several different tumor identities (Kessler et al. 2016). The functions of

Qijun Dai and Peipei Jiang contributed equally to this work.

Electronic supplementary material The online version of this article (doi:10.1007/s10571-016-0453-1) contains supplementary material, which is available to authorized users.

✉ Chengwei Duan
nt5621@126.com

✉ Lianxia Qu
qulianxiant@outlook.com

¹ Department of Orthopedics, Traditional Chinese Medicine Hospital of Haian County Affiliated Hospital, Nanjing University of Chinese Medicine of Hanlin College, Ninghai Road, Haian County 226600, Jiangsu Province, China

² Jiangsu Province Key Laboratory for Inflammation and Molecular Drug Target, Medical College of Nantong University, Nantong 226001, Jiangsu Province, China

IGFs are modulated by a family of binding proteins termed insulin-like growth factor binding proteins (IGFBPs). They exhibit different binding affinities and engage with IGFs and act as carriers, functioning as modulators of IGF activity, and transporting the IGFs out of the circulation to target tissues (Haramoto et al. 2014; Le Roith et al. 2001). IGFBPs have IGF-independent effects on cell functions like apoptosis (Mohan and Baylink 2002), which gains our attention.

The IGFBP family includes six high-affinity members designated IGFBP-1 through IGFBP-6 with variable functions and mechanisms of actions (Lund et al. 2014). Among the binding proteins, IGFBP-6 regulates IGF activity and may also have IGF-independent actions that bind preference for IGF-2 under normal physiological conditions (Raykha et al. 2013). It was therefore postulated that the major role of IGFBP-6 was to inhibit IGF-II actions and that this may be significant in the context of tumor inhibition (Bach 2005). Additionally, IGFBP-6 was found to suppress alkaline phosphatase (ALP) activity and the differentiation of both murine and human osteoblasts (Strohbach et al. 2008).

As IGFBPs are related to cell apoptosis, the role of IGFBPs in the pathophysiologic processes following ICH has still not been investigated. In present study, we focus on the effects exerted by IGFBP-6 in cells apoptosis in ICH. We examined the expression and distribution of IGFBP-6 in rat basal ganglia adjacent to the hematoma after ICH. We showed that IGFBP-6 participates in the pathogenesis of ICH, and inhibition of IGFBP-6 may be a promising strategy to treat brain injury.

Materials and Methods

Animals and the ICH Model

All animal care and surgical procedures were performed based on the Guide for the Care and Use of Laboratory Animals promulgated by the National Research Council in 1996, and supported by the Chinese National Committee to Use of Experimental Animals for Medical Purposes. Male Sprague–Dawley rats ($n = 50$, 6–8 weeks) with an average body weight of 250 g were used in this study. These rats were kept in a temperature-controlled environment (21 °C) on a 12 h light–dark cycle, with appropriate water and food supplied. ICH model was conducted according to a previous report with minor modifications (Xu et al. 2015). The rats were anesthetized with chloral hydrate, autologous blood, or saline (sham group). 50 μ L was injected into the right basal ganglia stereotactically at a rate of 10 μ L/min through a 26-gage needle (coordinates: 0.2 mm anterior, 5.5 mm ventral, and 3.5 mm lateral to the bregma, and concrete site of perihematoma was located at right

caudatum) using a microinfusion pump. The needle was kept still for 10 min after injection and then removed.

Behavioral Testing Procedures

Forelimb placing and corner turn tests were used to assess neurological deficits induced by ICH.

Forelimb Placing Test

Forelimb placing test was performed as described (Karabiyikoglu et al. 2004). The rats were held by torsos, allowing the forelimb to hang free. Testing of each forelimb was conducted by brushing the vibrissae on the corner edge of a countertop. Intact rats placed the forelimb quickly onto the countertop. Basing on the severity of injury, placing of the forelimb contralateral to the injury was impaired. During the experiments, every rat was tested 3 times for each forelimb. The percentage of trials in which the rat placed its left forelimb was calculated.

Corner Turn Test

Corner turn test was performed as described (Li et al. 2013). Rats proceed into a corner, whose angle was 30°. In order to exit the corner, the rats should turn to the left or the right; only the turns involving full rearing along either wall were involved (a total of eight per animal). Injured rats would show a tendency to turn to the side of the injury. The percentage of right turns was used as the corner turn score. After each turn, the rats were not picked up immediately, so that they would not develop an aversion for their prepotent turning response.

Cell Cultures and Stimulation

Rat pheochromocytoma (PC12) cells were obtained from the American Type Culture Collection (Rockville, MD) and were cultured in Dulbecco's modified Eagle's medium (DMEM) supplemented with 10% (v/v) fetal bovine serum and 1% penicillin/streptomycin at 37 °C under 5% CO₂ and 95% oxygen in humidified air. The medium was changed every 2 days. In order to explore apoptosis, PC12 cells were seeded onto 60-mm dishes and incubated in a low concentration of serum (1% horse serum) for 24 h prior to treatment with hemin (100 μ mol/L) for different time points.

Expression Plasmid and Transient Transfection

The Full-length IGFBP-6 and IGFBP-6-specific siRNAs were chemically synthesized by Genechem (Shanghai, China). Transfections were performed with the transfection reagent Lipofectamine 2000 (Invitrogen, Carlsbad, CA,

USA) according to the manufacturer's instructions. After incubation for 6 h, the medium was changed into DMEM containing 10% fetal bovine serum (Gibco-BRL, Grand Island, NY, USA). Transfected cells were used for the subsequent experiments 72 h after transfection.

Western Blotting

To obtain samples for Western blot, rats were sacrificed at 3, 6, 12 h, 1, 2, 3, 5, and 7 days after operation. Brain tissues surrounding the hematoma (extending 2 mm from the boundary of hematoma) and the counterparts from the contralateral side of the brain or the sham-operated group were dissected and flash-frozen at -80°C until use. In order to prepare lysates, frozen samples were weighed and minced with eye scissors in an ice bath. Then the tissues were homogenized in lysis buffer (1% NP-40, 50 mmol/L Tris, 1% SDS, 5 mmol/L EDTA, 1% sodium deoxycholate, 1% Triton-X100, 1 mmol/L PMSF, 10 $\mu\text{g}/\text{mL}$ aprotinin, and 1 $\mu\text{g}/\text{mL}$ leupeptin, $\text{pH} = 7.5$) and centrifuged at 12,000 rpm at 4°C for 20 min to collect the supernatant. After determination of its protein concentration with the Bradford assay (Bio-Rad), the resulting supernatant (50 μg of protein) was subjected to SDS–polyacrylamide gel electrophoresis (PAGE). The separated proteins were transferred to a polyvinylidene difluoride filter (PVDF) membrane by a transfer apparatus at 300 mA for 90 min. The membrane was then blocked with 5% nonfat milk or 5% bovine serum albumin, and then incubated with primary antibody against IGFBP-6 (rabbit, 1:200, Santa Cruz), Bax (rabbit, 1:500, Santa Cruz), Bcl-2 (mouse, 1:500, Santa Cruz), active caspase-3 (mouse, 1:500, Cell Signaling), and β -actin (mouse, 1:1000, Santa Cruz). At last, the membranes were incubated with secondary antibodies for 2 h and visualized with an enhanced chemiluminescence (ECL) kit (Pierce) or scanned with the Odyssey Infrared Imaging System (LI-COR Bioscience).

Immunohistochemistry

Tissues were subsequently cut at 5 μm with a cryostat and processed for immunohistochemistry analysis. Stereological methods were employed in the immunohistochemical evaluation. After the sections had been prepared, they were kept in an oven at 37°C for 60 min and rinsed twice with 0.01 M PBS for 5 min each. Then the sections were blocked by confining liquid consisting of 10% normal donkey serum, 1% bovine serum albumin (BSA), 0.3% Triton X-100, and 0.15% Tween-20 for 2 h at room temperature, and incubated with anti-IGFBP-6 antibody (rabbit, 1:100; Santa Cruz) overnight at 4°C , followed by incubation with the primary and the secondary antibodies for 20–30 min at 37°C and color reaction with a liquid mixture [0.02% diaminobenzidine tetrahydrochloride (DAB), 3% H_2O_2 and 0.1% PBS].

Finally, the sections were air-dried, dehydrated, and covered with coverslips. Slides were examined at $20\times$ or $40\times$ magnifications on a Leica light microscope (Germany). Cells with strong or moderate brown staining were considered as positive; otherwise, cells with no staining were regarded as negative. The mean assay of each group was used as the valuable result.

Immunofluorescent Staining

The frozen cross sections (5 μm) were prepared and examined. All sections were first blocked with 10% normal donkey serum blocking solution from the same species as the secondary antibody, containing 3% (w/v) BSA, 0.1% Triton X-100, and 0.05% Tween-20, for 2 h at room temperature to avoid non-specific staining. Then the sections were incubated with both primary antibodies for anti-IGFBP-6 (1:100, Santa Cruz,) and different cell markers as follows: NeuN (1:750, Chemicon), GFAP (1:200, Sigma), Iba1 (1:750, Santa Cruz), active caspase-3 (1:400, Cell Signaling) at 4°C overnight. A mixture of FITC-conjugated and TRITC-conjugated secondary antibodies was used for 2 h at 4°C . The stained sections were examined with a Leica fluorescence microscope (Germany).

Quantitative Analysis

Cells double labeled for IGFBP-6 and cell phenotypic markers used in the experiment were quantified in an unbiased manner. At least of 200 phenotype-specific marker-positive cells were counted adjacent to the hematoma in each section in order to identify the proportion of each phenotype-specific marker-positive cells expressing IGFBP-6. Then double-labeled cells for IGFBP-6 and NeuN were recorded. A total of three adjacent sections per animal were sampled. So did GFAP, Iba1.

Statistical Analysis

All data were analyzed with Stata 7.0 statistical software. All values are expressed as mean \pm SEM. Student's *t* test was used for pairwise comparisons. One-way ANOVA, with Tukey's post hoc test, was used for multiple comparisons. $P < 0.05$ was considered statistically significant. Each experiment consisted of at least three replicates per condition.

Results

The Changes of Neurological Deficits Following ICH

According to previous reports (Ke et al. 2015), behavior tests including forelimb placing and corner turn test were

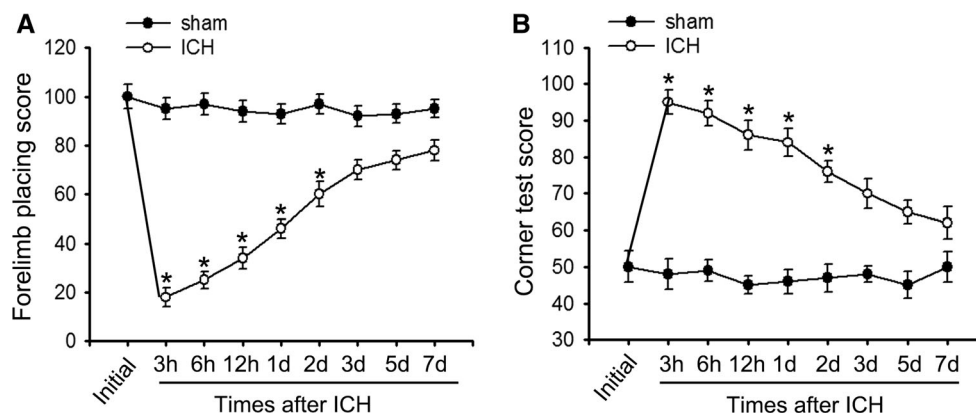


Fig. 1 Assessment and scores of behavioral tests at different time points on rats suffering from ICH. Corner turn testing (a) and forelimb placing scores (b) were displayed at various time points following ICH. The ICH group exhibited distinctly functional deficits compared with the sham-operated group over the first 3 days

(* $P < 0.05$, significantly different from the sham-operated group), but there was with no significant difference at baseline for 5 days later. Densitometric analysis data are presented as mean \pm SEM ($n = 3$, * $P < 0.05$)

performed to measure acute and chronic changes in sensorimotor function and plasticity of sham group and ICH group separately. As shown in Fig. 1, rat in ICH group was obviously worse impaired compared with the sham-operated group over the first 3 days (* $P < 0.05$), whereas by 5 days and thereafter, all rats had recovered neurological test scores.

Expression Changes of IGFBP-6 After ICH

To detect the IGFBP-6 expression after ICH, Western blot was applied to investigate the temporal levels of IGFBP-6 in rat basal ganglia around the hematoma at different time points. As shown in Fig. 2a, b, the expression of IGFBP-6 was relatively low in the sham group, progressively increased from 3 h after ICH, reached the peak at day 2, and then gradually decreased thereafter. By the way, we also detected IGFBP-6 protein expression in the contralateral brain, but failed to find any significant fluctuations (data not shown).

Expression and Distribution of IGFBP-6 Immunoreactivity

To further explore the upregulation of IGFBP-6 after ICH, immunohistochemistry staining was carried out on the brain tissues at 2 days following ICH to detect the variation and distribution of IGFBP-6. Obviously, ICH group showed stronger staining of IGFBP-6 (Fig. 3e, f), compared with the contralateral (Fig. 3c, d) and the sham group (Fig. 3a, b). Additionally, no positive signal was observed in the negative control (Fig. 3g). Quantitative analysis showed that there was significant increase of IGFBP-6-expressing cells after ICH around hematoma ($P < 0.05$) (Fig. 3h).

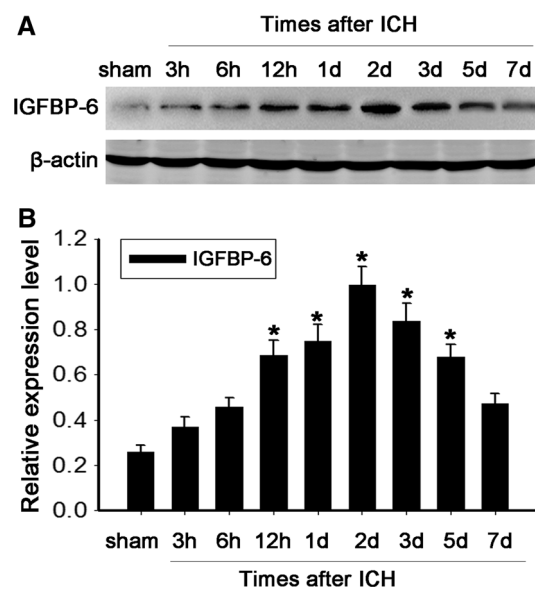
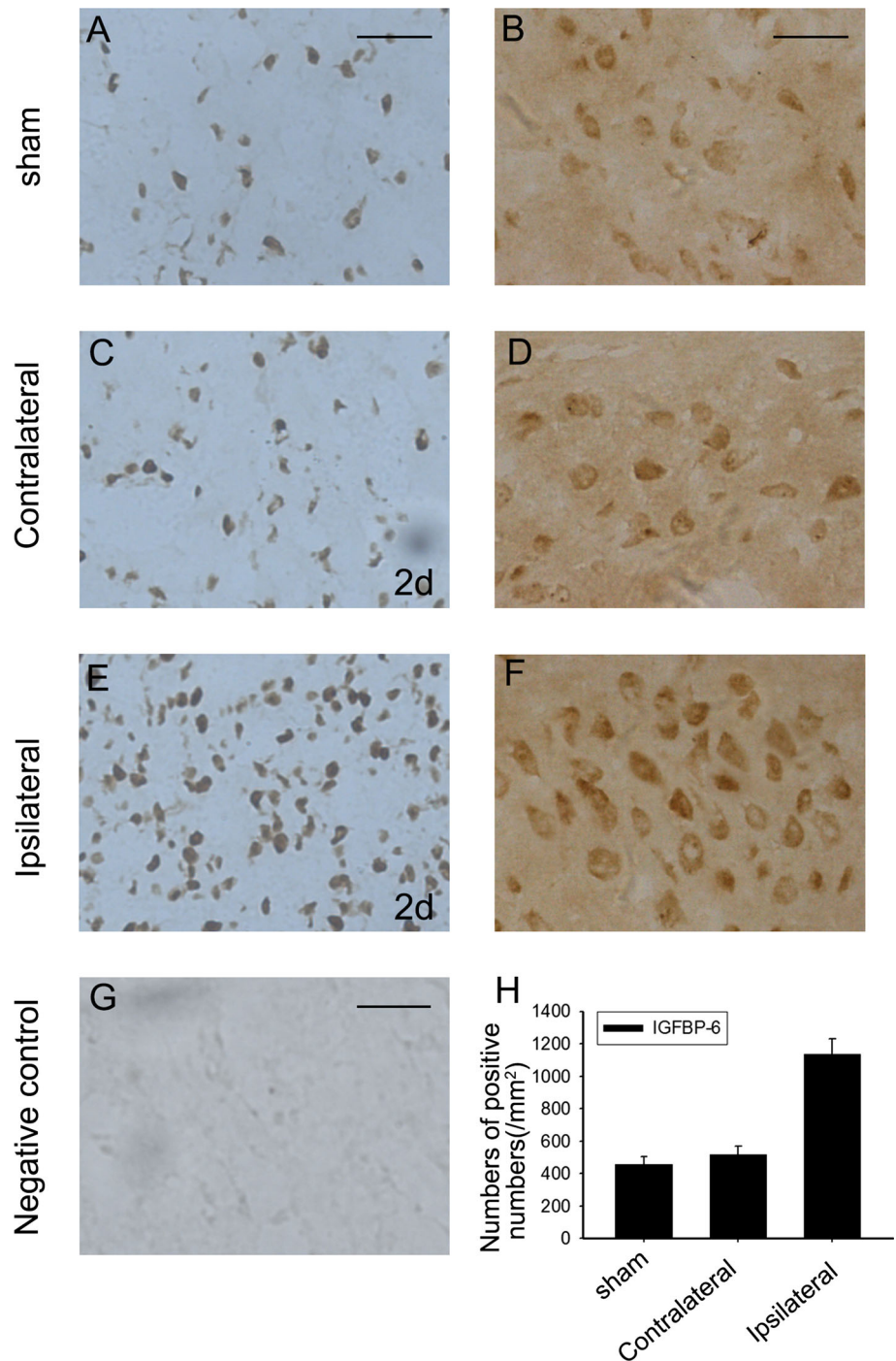


Fig. 2 Expression profiles of IGFBP-6 around the hematoma at each time point after ICH by Western blot analysis. The number of samples evaluated by immunohistochemical staining was 3 from each group. The expression of IGFBP-6 was relatively low in the sham group, however, upregulated gradually following ICH, peaked at day 2 and declined thereafter (a). The bar graph indicated the density of IGFBP-6 versus β -actin at each time point (b). Data are presented as mean \pm SEM ($n = 3$, * $P < 0.05$)

Co-Localization of IGFBP-6 with Different Cellular Markers by Double Immunofluorescent Staining

To further identify the cell types in the brain that express IGFBP-6, double-labeling immunofluorescent staining was employed with distinct cell-specific markers, such as NeuN, GFAP, and Iba1, which represent neurons, astrocytes, and microglia, respectively. In the sham-operated group, the staining of IGFBP-6 was merely restricted to NeuN-positive

Fig. 3 Expression and distribution of IGFBP-6 immunoreactivity. The number and intensity of IGFBP-6 positive cells had significantly increased 2 days in the ipsilateral group (e, f) compared with the sham-control group (a, b) or the contralateral group (c, d). No staining was detected in the negative control sections (g). Quantitative analysis of IGFBP-6-positive cells in the ipsilateral group at 2 days after ICH ($*P < 0.05$) compared with the sham-control group (h). Error bars represent SEM. Scale bar left column 100 μm ; right column 50 μm



cells. Following ICH, microscopy indicated that IGFBP-6 was specifically expressed in neurons (Fig. 4c, f), instead of in astrocytes (Fig. 4h, l) or microglia (Fig. 4n, r).

IGFBP-6 Relevant to Neuronal Apoptosis after ICH

As shown above, increased immunoreactivity of IGFBP-6 was observed in neurons. Previous studies have proved that neuronal apoptosis was a significant event surrounding

hematoma in ICH (Liu et al. 2016). Therefore, it was speculated that IGFBP-6 was involved in neuronal apoptosis. To confirm our assumption, Western blot analysis was carried out to examine the expression of active caspase-3 (a marker of apoptosis). As expected, the expression profiles of active caspase-3 changed after ICH, and peaked at day 2 (Fig. 5a, b), which was relevant with the expression of IGFBP-6 in a time-dependent manner. Furthermore, double immunofluorescent staining displayed that the

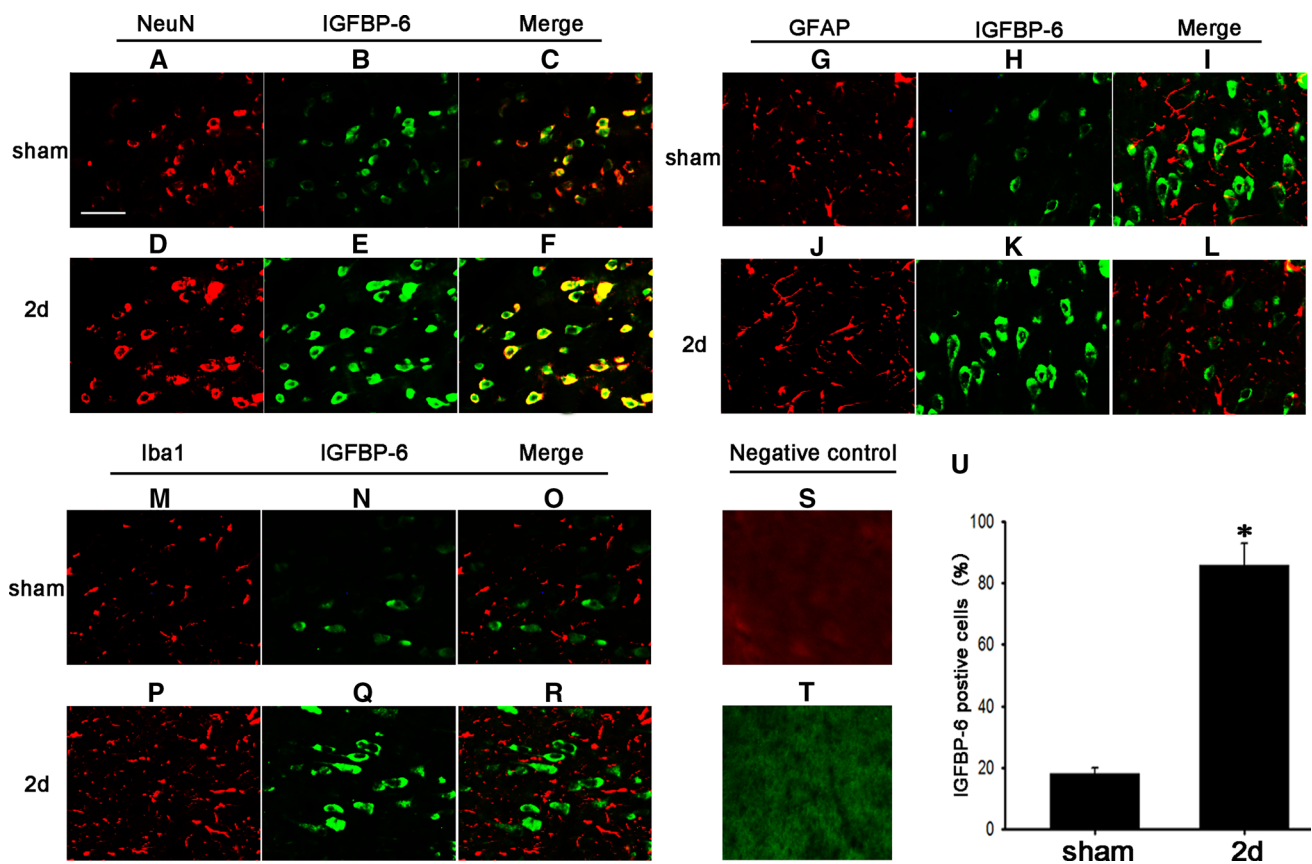


Fig. 4 Double immunofluorescence staining for IGFBP-6 and different phenotype-specific markers in brain caudate putamen surrounding the hematoma. Sections labeled with IGFBP-6 (green **b, h, n, e, k, q**) and different cell markers, including neuron marker (red **a, d**, NeuN), astrocyte marker (red **g, j**, GFAP), and microglia marker (red **m, p**, Iba1). The yellow color visualized in the merged images represented co-localization of IGFBP-6 with different phenotype-

specific markers (**c, i, o**). Co-staining of IGFBP-6 with different phenotype-specific markers in the sham-operated group is shown (**f, l, r**). No positive signals were found in the negative control (**s, t**). Quantitative analysis of NeuN positive cells expressing IGFBP-6 (%) in the sham group and 2 days after ICH (**u**). * $P < 0.05$, indicate significant difference compared with sham-operated group. Error bars represent SEM. Scale bars 50 μm (**a–t**)

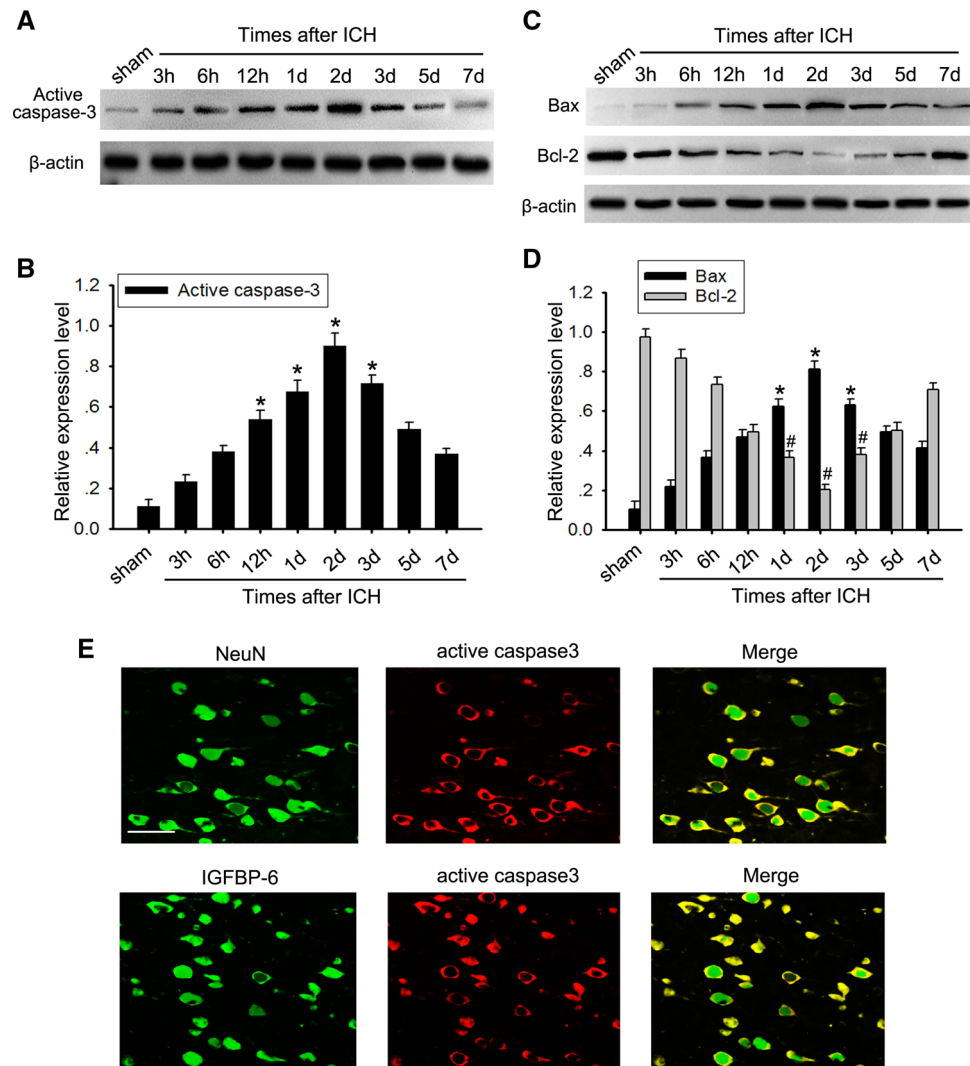
active caspase-3 not only located in neurons, but also co-located with IGFBP-6 at day 2 after ICH around the hematoma (Fig. 5e). To further detect the association between IGFBP-6 and neuronal apoptosis, we also examined the expression profiles of Bax and Bcl-2. As shown in Fig. 5b, c, Bax were upregulated and the expression was also parallel with that of IGFBP-6 and active caspase-3 after ICH. Meanwhile, the expression of Bcl-2 was downregulated, which was opposite with those of IGFBP-6, active caspase-3, and Bax. Taken these results together, we suggested that IGFBP-6 may participate in the process of neuronal apoptosis in a caspase-dependent way following ICH.

IGFBP-6 Regulates Cellular Apoptosis In Vitro

To further test the role of IGFBP-6 playing in neuronal apoptosis after ICH, hemin-induced apoptosis model was built in PC12 cells (Shen et al. 2015). First, siRNA was employed to knock down IGFBP-6 expression in PC12

cells. The control-siRNA, non-specific RNA, and si-IGFBP-6 were transiently transfected into PC12 cells for 48 h, and the interference efficiency of IGFBP-6 siRNA was examined using Western blot analysis. It turned out that the expression of IGFBP-6 was inhibited obviously by IGFBP-6 siRNA compared with control-siRNA or non-specific RNA (Fig. 6a, b). In addition, the expression of active caspase-3 and Bax was significantly downregulated accompanied by the upregulation of Bcl-2 in PC12 cells which transfected with siRNA targeting IGFBP6 compared with non-specific siRNA cells with or without hemin stimulation (Fig. 6c, d). To further confirm the results, immunofluorescent staining of PC12 cells revealed that silence of IGFBP-6 reduced the expression of active caspase-3 and nuclear condensation of these cells after hemin treatment (Fig. 6e). In addition, we also employed another IGFBP-6 siRNA that was transfected in SH-SY5Y cell to further confirm our results. As shown in Fig.S1 A and B, the expression of IGFBP-6 was effectively suppressed by IGFBP-6 siRNA-2. Moreover, we also detected the

Fig. 5 Correlations of IGFBP-6 with cell apoptosis following ICH. The expression of active caspase-3 and Bax increased, peaked at day 2 following ICH (a). The expression of Bcl-2 decreased after ICH and reached valley at 2 days (c). The bar graphs indicated the relative density of active caspase-3, Bax, and Bcl-2 versus β -actin at each time point (b, d). Data are presented as mean \pm SEM. ($n = 3$, *, # $P < 0.05$, significantly distinct from the sham-controlled group). Double immunofluorescent staining showed co-staining of IGFBP-6 (green) and NeuN (green) with active caspase-3 (red) in the section at day 2 after ICH (e). Scale bar 25 μ m (e)



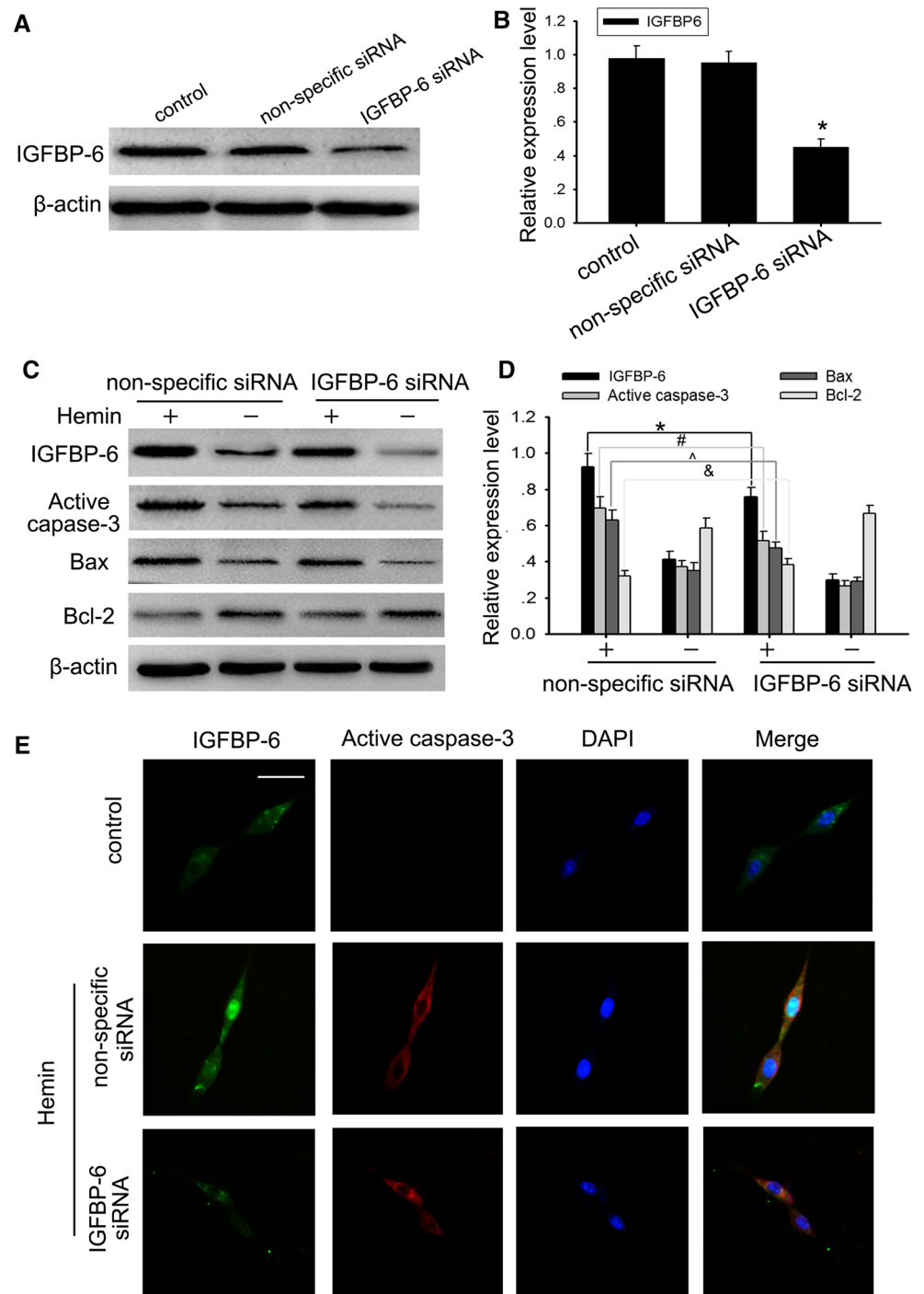
expression of IGFBP-6, active caspase-3, Bax, and Bcl-2 in hemin-induced apoptosis model. As expected, the expression of active caspase-3 and Bax was significantly decreased accompanied by the increase of Bcl-2 in SH-SY5Y cells which transfected with IGFBP-6-siRNA-2 compared with non-specific siRNA cells with or without hemin stimulation (Fig. S1C, D). Immunofluorescent staining of SH-SY5Y cells was also performed. The results were similar with that in PC12 cells (Fig. S1E). overall, our findings demonstrated that IGFBP-6 might exert its proapoptotic activity in neurons via regulating the caspase-3/Bax/Bcl-2 pathway, and thus participated in ICH.

Discussion

Intracerebral hemorrhage (ICH) is a perplexing condition with high mortality and no treatment beyond supportive care. A major portion of the injurious process is taken place

during the hours following the development of hematoma (Behrouz 2016). Development of treatment goals for critical care, and new sequences of care and specialty practice can only improve outcome after intracerebral hemorrhage (Xu et al. 2015). It is important to gain a better understanding of the molecular and cellular mechanisms underlying ICH. Based on the volume of bleeding and the predilection site in clinical scenarios, an ICH rat model was established to further explore the exact role of IGFBP-6 in ICH. Our data show that IGFBP-6 protein levels were rapidly upregulated and reach the peak at 2 day in the perihematomal region after ICH. Importantly, double-label immunofluorescence suggested that IGFBP-6 was widely distributed in neurons after ICH, rather than in astrocytes or oligodendrocytes. It reminded us that the upregulation of IGFBP-6 might be associated with neuronal apoptosis after ICH. As expected, we found that the expression patterns of Bax, Bcl-2, and active caspase-3 consistent with that of IGFBP-6 in vivo and in vitro. Furthermore, silencing of

Fig. 6 Modulations of IGFBP-6 on cell apoptosis in vitro. Western blot showed siRNA silenced IGFBP-6 in PC12 cells (a); the bar chart indicated the density of IGFBP-6 versus β -actin (b). The knockdown of IGFBP-6 induced decreasing levels of active caspase-3 and Bax and had upregulation of Bcl-2 expression (c). The bar graph indicated the relative density of IGFBP-6, active caspase-3, Bax, and Bcl-2 versus β -actin (d). Data are presented as mean \pm SEM. ($n = 3$, *, #, ^, & $P < 0.05$, significantly different from the control-siRNA-treated group). Immunofluorescent analysis of the co-localization between IGFBP-6 and active caspase-3 in control, non-specific siRNA, or IGFBP-6 siRNA-transfected PC12 cells after hemin treatment (e)



IGFBP-6 by siRNA in PC12 cells can suppress hemin-induced expression of Bax, Bcl-2, and active caspase-3. These results suggest that IGFBP-6 might play a vital role in modulating the progression of neuronal apoptosis in this model.

CNS pathological states are associated with the IGF system (Lioutas et al. 2015; Madathil and Saatman 2015). The insulin superfamily of peptides is phylogenetically ancient and has emerged as crucial in the growth and

development of the CNS (Fernandez and Torres-Aleman 2012). IGFBPs are important in the modulation of IGF-1 activity, binding to IGF-1 with consequent implications for its localization and bioavailability (Clemmons et al. 1995; Dyer et al. 2016). There are six high-affinity IGFBPs, with IGFBP-2 and IGFBP-4 the most abundantly expressed in the CNS (Fernandez and Torres-Aleman 2012; Konermann et al. 2013). IGFBP expression is highest in the developing brain, with expression patterns maintained in the adult

brain. They serve as an important point of biological modification of IGF-1 signaling in the CNS (Fernandez and Torres-Aleman 2012).

Numerous observations suggest that, in several neurodegenerative diseases or related, IGF family affected neurons display an early impairment in the brain (Annunziata et al. 2011). However, the exact role of IGFBP-6 in these processes remains poorly understood. As reported, IGFBP-6 had its involvement in hypoxic-ischemic injury in rat brain (Beilharz et al. 1998). Consequently, on the basis of previous studies on IGFBP-6, we wonder whether IGFBP-6 can induce neuronal/cellular activities through some other ways, such as promoting neuronal apoptosis after ICH. Little can be done to alleviate the initial damage. It becomes clear that neuronal apoptosis is the predominant process of ICH-mediated brain injury. Accumulating evidence suggests apoptotic mechanisms in delayed tissue loss after brain injury, such as regulation of pro-apoptotic proteins which mediate caspase-dependent or caspase-independent cell death. Our data suggest that pro-apoptotic proteins include Bax, Bcl-2 and active caspase-3 that are upregulated in rat ICH models. Moreover, increase of active caspase-3 level after hematoma indicates that neuronal apoptosis occurred. Double immunofluorescence staining in the rat cerebral cortex showed that active caspase-3 co-localized well with IGFBP-6 in neurons. Meanwhile, experimental data suggest that IGFBP-6 represents one of the pro-apoptotic aspects in ICH. Therefore, our results indicated that upregulation of IGFBP-6 might be positively associated with neuronal apoptosis following ICH.

In present study, we demonstrate the association of IGFBP-6 in neuronal apoptosis with ICH. Inhibition of IGFBP-6 and concomitant activation of pro-apoptosis signaling therefore can be an attractive therapeutic strategy for the treatment towards ICH. However, it is imperative that further investigation should be carried out to provide more convincing data for IGFBP-6 related with neuronal apoptosis after brain trauma.

Authors' Contributions CD and LQ designed experiments; QD and PJ carried out experiments; YG, LZ, HD and ZY analyzed experimental results; HL analyzed sequencing data and developed analysis tools; XM wrote the manuscript.

Compliance with Ethical Standards

Conflict of interest The authors declare no conflict of interest.

References

- Annunziata M, Granata R, Ghigo E (2011) The IGF system. *Acta Diabetol* 48:1–9. doi:10.1007/s00592-010-0227-z
- Aronowski J, Zhao X (2011) Molecular pathophysiology of cerebral hemorrhage: secondary brain injury. *Stroke* 42:1781–1786. doi:10.1161/STROKEAHA.110.596718
- Bach LA (2005) IGFBP-6 five years on; not so ‘forgotten’? *Growth Horm IGF Res* 15:185–192. doi:10.1016/j.ghir.2005.04.001
- Behrouz R (2016) Re-exploring tumor necrosis factor alpha as a target for therapy in intracerebral hemorrhage. *Transl Stroke Res*. doi:10.1007/s12975-016-0446-x
- Beilharz EJ et al (1998) Co-ordinated and cellular specific induction of the components of the IGF/IGFBP axis in the rat brain following hypoxic-ischemic injury. *Brain Res Mol Brain Res* 59:119–134
- Chao W, D’Amore PA (2008) IGF2: epigenetic regulation and role in development and disease. *Cytokine Growth Factor Rev* 19:111–120. doi:10.1016/j.cytogfr.2008.01.005
- Chen X, Shen J, Wang Y, Chen X, Yu S, Shi H, Huo K (2015) Up-regulation of c-Fos associated with neuronal apoptosis following intracerebral hemorrhage. *Cell Mol Neurobiol* 35:363–376. doi:10.1007/s10571-014-0132-z
- Clemmons DR, Busby WH, Arai T, Nam TJ, Clarke JB, Jones JI, Ankrapp DK (1995) Role of insulin-like growth factor binding proteins in the control of IGF actions. *Prog Growth Factor Res* 6:357–366
- Dyer AH, Vahdatpour C, Sanfeliu A, Tropea D (2016) The role of insulin-like growth factor 1 IGF-1 in brain development maturation and neuroplasticity. *Neuroscience* 325:89–99. doi:10.1016/j.neuroscience.2016.03.056
- Fernandez AM, Torres-Aleman I (2012) The many faces of insulin-like peptide signalling in the brain *Nature reviews. Neuroscience* 13:225–239. doi:10.1038/nrn3209
- Hammond MD et al (2014) CCR2+ Ly6C(hi) inflammatory monocyte recruitment exacerbates acute disability following intracerebral hemorrhage. *J Neurosci* 34:3901–3909. doi:10.1523/JNEUROSCI.4070-13.2014
- Haramoto Y, Oshima T, Takahashi S, Ito Y (2014) Characterization of the insulin-like growth factor binding protein family in *Xenopus tropicalis*. *Int J Dev Biol* 58:705–711. doi:10.1387/ijdb.150032yi
- Karabiyikoglu M, Hua Y, Keep RF, Ennis SR, Xi G (2004) Intracerebral hirudin injection attenuates ischemic damage and neurologic deficits without altering local cerebral blood flow. *J Cereb Blood Flow Metab* 24:159–166. doi:10.1097/01.WCB.0000100062.36077.84
- Ke K et al (2015) Up-regulation of Glis2 involves in neuronal apoptosis after intracerebral hemorrhage in adult rats. *Cell Mol Neurobiol* 35:345–354. doi:10.1007/s10571-014-0130-1
- Kessler SM, Haybaeck J, Kierner AK (2016) Insulin-like growth factor 2—the oncogene and its accomplices. *Curr Pharm Des* 22(39):5948–5961
- Konermann A, Lossdorfer S, Jager A, Chen Y, Gotz W (2013) Autoregulation of insulin-like growth factor 2 and insulin-like growth factor-binding protein 6 in periodontal ligament cells in vitro. *Ann Anat* 195:527–532. doi:10.1016/j.aanat.2013.10.001
- Le Roith D, Bondy C, Yakar S, Liu JL, Butler A (2001) The somatomedin hypothesis. *Endocr Rev* 22:53–74. doi:10.1210/edrv.22.1.0419
- Leclerc JL, Lampert AS, Diller MA, Immergluck JB, Dore S (2015) Prostaglandin E2 EP2 receptor deletion attenuates intracerebral hemorrhage-induced brain injury and improves functional recovery. *ASN Neuro*. doi:10.1177/1759091415578713
- Li L et al (2013) Up-regulation of NFATc4 involves in neuronal apoptosis following intracerebral hemorrhage. *Cell Mol Neurobiol* 33:893–905. doi:10.1007/s10571-013-9955-2
- Lioutas VA, Alfaro-Martinez F, Bedoya F, Chung CC, Pimentel DA, Novak V (2015) Intranasal insulin and insulin-like growth factor

- 1 as neuroprotectants in acute ischemic stroke. *Transl Stroke Res* 6:264–275. doi:[10.1007/s12975-015-0409-7](https://doi.org/10.1007/s12975-015-0409-7)
- Liu C et al (2016) Increased expression of ubiquitin-specific protease 4 participates in neuronal apoptosis after intracerebral hemorrhage in adult rats. *Cell Mol Neurobiol*. doi:[10.1007/s10571-016-0375-y](https://doi.org/10.1007/s10571-016-0375-y)
- Lund J, Sondergaard MT, Conover CA, Overgaard MT (2014) Heparin-binding mechanism of the IGF2/IGF-binding protein 2 complex. *J Mol Endocrinol* 52:345–355. doi:[10.1530/JME-13-0184](https://doi.org/10.1530/JME-13-0184)
- Madathil SK, Saatman KE (2015) IGF-1/IGF-R signaling in traumatic brain injury. In: Kobeissy FH (ed) *Brain neurotrauma: molecular, neuropsychological, and rehabilitation aspects*. CRC Press/Taylor & Francis, Boca Raton, FL
- Malandrakis EE et al (2016) DNA damage and differential gene expression associated with physical stress in gilthead seabream (*Sparus aurata*). *Gen Comp Endocrinol*. doi:[10.1016/j.ygcen.2016.07.009](https://doi.org/10.1016/j.ygcen.2016.07.009)
- Mohan S, Baylink DJ (2002) IGF-binding proteins are multifunctional and act via IGF-dependent and -independent mechanisms. *J Endocrinol* 175:19–31
- Raykha C, Crawford J, Gan BS, Fu P, Bach LA, O’Gorman DB (2013) IGF-II and IGFBP-6 regulate cellular contractility and proliferation in Dupuytren’s disease. *Biochim Biophys Acta* 1832:1511–1519. doi:[10.1016/j.bbadis.2013.04.018](https://doi.org/10.1016/j.bbadis.2013.04.018)
- Shen J, Liu Y, Song Y, Li L, Duan C, Zhou Y, Ke K (2015) CHMP4B, ESCRT-III associating protein, associated with neuronal apoptosis following intracerebral hemorrhage. *Brain Res* 1597:1–13. doi:[10.1016/j.brainres.2014.11.043](https://doi.org/10.1016/j.brainres.2014.11.043)
- Strohbach C, Kleinman S, Linkhart T, Amaal Y, Chen ST, Mohan S, Strong D (2008) Potential involvement of the interaction between insulin-like growth factor binding protein (IGFBP)-6 and LIM mineralization protein (LMP)-1 in regulating osteoblast differentiation. *J Cell Biochem* 104:1890–1905. doi:[10.1002/jcb.21761](https://doi.org/10.1002/jcb.21761)
- Xi G, Keep RF, Hoff JT (2006) Mechanisms of brain injury after intracerebral haemorrhage. *Lancet Neurol* 5:53–63. doi:[10.1016/S1474-4422\(05\)70283-0](https://doi.org/10.1016/S1474-4422(05)70283-0)
- Xu Z et al (2015) USP11, deubiquitinating enzyme, associated with neuronal apoptosis following intracerebral hemorrhage. *J Mol Neurosci*. doi:[10.1007/s12031-015-0644-0](https://doi.org/10.1007/s12031-015-0644-0)